www.elsevier.com/locate/developmentalbiology

Transcriptome profiling of the cardiac neural crest reveals a critical role for MafB

Saori Tani-Matsuhana, Felipe Monteleone Vieceli, Shashank Gandhi, Kunio Inoue, Marianne E. Bronner

PII: S0012-1606(18)30236-7
DOI: https://doi.org/10.1016/j.ydbio.2018.09.015
Reference: YDBIO7863

To appear in: *Developmental Biology*

Received date: 1 April 2018
Revised date: 5 September 2018
Accepted date: 15 September 2018

Cite this article as: Saori Tani-Matsuhana, Felipe Monteleone Vieceli, Shashank Gandhi, Kunio Inoue and Marianne E. Bronner, Transcriptome profiling of the cardiac neural crest reveals a critical role for MafB, *Developmental Biology,* https://doi.org/10.1016/j.ydbio.2018.09.015

Transcriptome profiling of the cardiac neural crest reveals a critical role for MafB

Saori Tani-Matsuhana[a,b1], Felipe Monteleone Vieceli[a1], Shashank Gandhi[a], Kunio Inoue[b], Marianne E. Bronner[a*]

[a]Division of Biology and Biological Engineering, California Institute of Technology, Pasadena, CA 91125, USA

[b]Department of Biology, Graduate School of Science, Kobe University, Kobe, 657-8501, Japan

*Correspondence to: mbronner@caltech.edu

ABSTRACT

The cardiac neural crest originates in the caudal hindbrain, migrates to the heart, and contributes to septation of the cardiac outflow tract and ventricles, an ability unique to this neural crest subpopulation. Here we have used a *FoxD3* neural crest enhancer to isolate a pure population of cardiac neural crest cells for transcriptome analysis. This has led to the identification of transcription factors, signaling receptors/ligands, and cell adhesion molecules upregulated in the early migrating cardiac neural crest. We then functionally tested the role of one of the upregulated transcription factors, *MafB*, and found that it functions as a regulator of *Sox10* expression specifically in the cardiac neural crest. Our results not only reveal the genome-wide profile of early migrating cardiac neural crest cells, but also provide molecular insight into what makes the cardiac neural crest unique.

Keywords

MafB; cardiac neural crest; RNA-Seq; Sox10E2; transcription factor

INTRODUCTION

The neural crest is an embryonic cell population, characterized by broad migratory and differentiation ability. Arising within the central nervous system shortly after neural tube closure,

1 These authors contributed equally

neural crest cells undergo an epithelial to mesenchymal transition and begin migrating along stereotypic pathways to diverse sites throughout the body. Upon cessation of migration, they differentiate into numerous derivatives including elements of the craniofacial skeleton, peripheral nervous system, connective tissue and melanocytes. Just as the nervous system is patterned along the body axis, neural crest cells have different developmental capabilities depending upon their site of origin within the neural tube. For example, only cranial neural crest cells contribute to bone and cartilage of the face whereas neural crest cells emerging at spinal cord levels fail to do so (Le Douarin, 1982; Simoes-Costa and Bronner, 2016).

Arising in the dorsal neural tube just caudal to the cranial region is the “cardiac” neural crest, a particularly interesting region which is the only neural crest population that contributes to the cardiovascular system. Based on fate mapping studies using quail-chick chimeras, the cardiac neural crest has been shown to originate in the neural tube from the middle of the otic vesicle to the 3rd somite, corresponding to rhombomeres 6, 7 and 8 (Hutson and Kirby, 2007; Kirby et al., 1985). From this site of origin, these cells migrate through pharyngeal arches 3, 4 and 6 to contribute to elements of the cardiovascular system, including the aortic arch arteries and septum of the outflow tract into aortic and pulmonary trunks (Kirby et al., 1983; Le Lièvre and Le Douarin, 1975). They also contribute to the valves, ventricular septae and the cardiac ganglion (Kirby and Stewart, 1983; Waldo et al., 1998).

Surgical ablation of the cardiac neural crest cell population results in a severe heart defect known as persistent truncus arteriosus (Besson et al., 1986; Kirby et al., 1985; Nishibatake et al., 1987). This is caused by the absence of truncal and aorticopulmonary septa, resulting in fusion of the pulmonary and aortic blood vessels. Congenital heart defects, including failure in septation or abnormalities of the great arteries, are the most common human birth defects observed in the general population (Neeb et al., 2013). Importantly, other neural crest populations are unable to rescue the effects of cardiac crest ablation, even when grafted in its place at stage HH10 (Kirby, 1989). Thus, the unique developmental potential of the cardiac neural crest to contribute to the cardiovascular system, that is lacking in other neural crest populations, seems to be determined at early developmental stages.

Neural crest cell formation is guided by a gene regulatory network (GRN) comprised of a combination of transcription factors and signaling molecules (Meulemans and Bronner-Fraser, 2004; Simões-Costa and Bronner, 2015). One means of demonstrating direct connections within this GRN has been to identify enhancers and their inputs for neural crest genes like *Sox10* and *FoxD3* (Betancur et al., 2010; Simões-Costa et al., 2012). These have been best characterized for the cranial neural crest. However, the gene regulatory circuit that imbues the cardiac neural crest with its singular abilities remains a mystery.

To understand the molecular mechanisms that render the cardiac neural crest unique, we sought to identify transcription factors and other genes highly upregulated in this cell population and determine their regulatory relationships. To this end, in the present study, we have used a *FoxD3* neural crest enhancer that drives expression of GFP in the neural crest to isolate a pure population of early migrating cardiac neural crest cells for transcriptional profiling. This has led to the identification of transcription factors, signaling receptors and ligands, as well as cell adhesion molecules amongst other genes that are upregulated in the early migrating cardiac neural crest. We then functionally tested the role of the transcription factor MafB in the cardiac neural crest. MafB knockdown affects the cardiac neural crest stream and causes reduction in expression of *Sox10*, *Krox20* and *MafB* itself. Furthermore, MafB appears to regulate expression of a *Sox10* enhancer in the cardiac neural crest. Taken together, the results reveal a novel role for MafB in cardiac neural crest cells.

RESULTS

FoxD3 NC2:EGFP reporter enables isolation of a pure population of cardiac neural crest cells for transcriptome profiling

FoxD3 is a neural crest specifier gene expressed in the pre-migratory and early migrating neural crest. The *FoxD3* enhancer NC2 drives expression in neural crest cells emerging posterior to rhombomere 4 (Simões-Costa et al., 2012). Therefore, we took advantage of this enhancer to drive GFP expression in cardiac neural crest cells. To this end, we electroporated the NC2:EGFP

construct into Hamburger and Hamilton (HH) stage 4 chicken embryos and incubated them until HH12, by which time cardiac neural crest migration had initiated (Fig. 1A,B). To confirm neural crest identity of the GFP-expressing cells, we performed immunostaining with HNK-1 and anti-GFP antibodies on transverse sections posterior to the otic vesicle. The results showed that the majority of HNK-1+ cells expressed GFP, which was only present in HNK-1+ cells with the exception of pre-migratory neural crest cells still associated with the dorsal neural tube (Fig. 1C).

With an eye toward identifying transcription factors and signaling molecules upregulated in the cardiac neural crest, we performed transcriptome analysis of this cell population. Because the NC2 enhancer also drives expression further caudally in the trunk, we dissected the embryonic region posterior to the otic vesicle to the 3rd somite (Fig. 1B), dissociated the tissue and sorted GFP-positive cells to obtain a population of pure migrating cardiac neural crest cells (Fig. 1D). RNA was extracted, reverse transcribed and amplified for library preparation and sequencing. We compared the RNA-seq data from cardiac neural crest cells with the GFP-negative cell population from the same embryonic region. The results revealed a list of 677 genes (Supplemental Table 1) that are enriched and 721 (Supplemental Table 2) that are depleted in early migrating cardiac neural crest cells, compared with the GFP-negative population (Fig. 1E).

To identify gene sets specifically enriched in cardiac neural crest cell and/or shared with other neural crest population, we compared the lists of genes upregulated in the cardiac and the cranial population, the latter from previous studies (Simões-Costa et al., 2014). Comparative analysis revealed that, amongst the list of genes upregulated in either of these neural crest populations, 570 genes are specifically enriched in the cardiac crest, 1074 genes unique to the cranial neural crest cells, and 107 genes shared by both populations (Fig. 1F). Of these, 30 transcriptional regulators were specific to the cardiac cells, 82 specific to the cranial, and 17 shared by both populations (Fig. 1F). Protein classification of the cardiac-enriched genes revealed a high frequency of nucleic acid binding, enzymatic and transcription factor activity in the encoded proteins (Fig. 1H). Functional annotation clustering revealed enrichment of terms related to translation and RNA processing, suggesting that post-transcriptional regulation is an important

aspect of the biology of migrating cardiac neural crest cells. The presence of genes related to cardiomyopathies highlights the essential contribution of these cells to heart development (Fig. 1I). In particular, this analysis revealed 34 transcription factors, 14 signaling molecules, 18 receptors, and 6 cell adhesion molecules upregulated in the early migrating cardiac neural crest.

Identification of novel players in migrating cardiac neural crest cells

To validate the gene set enriched in our transcriptome analysis of cardiac neural crest relative to surrounding tissues, we performed whole mount *in situ* hybridization on embryos at early stages of cardiac neural crest migration (HH12/13), focusing on transcription factors and signaling molecules. 14 of 20 genes tested showed expression in the cardiac neural crest streams (Fig. 2 and Supplemental Fig. 1). These included known neural crest factors, such as *CXCR4, Ret, Snail2, Sox10*, as well as novel players, such as *Dlx5 and Nrip1*, whose expression was not previously associated with the cardiac neural crest (Fig. 2). Transverse sections caudal to the otic vesicle and immunostaining with HNK-1 confirmed cardiac neural crest expression (Supplemental Fig. 1).

The transcription factor *MafB,* previously best known for its expression and function in rhombomeres 5 and 6, was amongst the highest upregulated genes in the cardiac neural crest (Fig. 1G). Consistent with previous reports (Eichmann et al., 1997; Lecoin et al., 2004), we first observed *MafB* expression in rhombomeres 5 and 6 at stage HH10 and expression was maintained not only in the rhombomeres, but also in cardiac neural crest cells at stage HH13 (Fig. 2A and Supplemental Fig. 2A,B). Neural crest expression was confirmed in transverse sections immediately caudal to the otic vesicle (Supplemental Fig. 2C). We further confirmed the identity of *MafB*-positive cells in the rhombomeres and cardiac neural crest using double fluorescence in situ hybridization of *MafB* and *Krox20 (also known as Egr2)*, another gene selectively expressed in the hindbrain and the associated neural crest cells (Schneider-Maunoury et al., 1993). *MafB* and *Krox20* are expressed in rhombomeres 5/6 and rhombomeres 3/5, respectively, and our results clearly show that expression of the two transcription factors overlaps in the cardiac neural crest stream emanating from rhombomere 5 (Fig. 2B).

Loss of MafB reduces the cardiac neural crest stream

As *MafB* function was not previously reported in the cardiac neural crest, we next sought to examine its role by using a FITC-tagged translation-blocking morpholino (MO) for loss-of-function experiments (Fig. 3A). To demonstrate MO efficacy, we compared the ability of MafB versus control MO to block expression of a construct containing the truncated 5' UTR and CDS of *MafB*, including the MO recognition sequence, driving expression of *RFP* (Supplemental Fig. 3A). Control MO was electroporated onto one side of the embryo and MafB MO onto the contralateral side (Supplemental Fig. 3B). The results show that the translation blocking MO eliminates reporter expression whereas control MO has no effect (Supplemental Fig. 3C-E).

To test the effects of MafB loss on cardiac neural crest development, we electroporated the translation-blocking MOs into the right side of HH4 chick embryos, using the left side as an internal control (Fig. 3B). Electroporated embryos were incubated until stage HH12, fixed and immunostained with the HNK-1 antibody to detect migrating neural crest cells. To allow comparison of phenotypes from control and MafB-depleted embryos, these were classified according to the severity and grouped as severe, strong, mild or none (Supplemental Fig. 4A). After MafB knockdown, HNK-1 signal was greatly reduced in cardiac neural crest cells when compared to either non-transfected contralateral controls or embryos electroporated with a control MO, whereas the cranial neural crest was unaffected (Fig. 3C-F and Supplemental Fig. 4B). As a second means of performing MafB knockdown, we created two dominant negative constructs: one in which the N-terminal acidic domain that functions for transactivation (1-194 amino acid) was removed (MafBΔN) and a second composed of MafBΔN fused to the Engrailed repressor domain (EnR; Conlon et al., 1996) (MafBΔN-EnR; Fig. 3A and Supplemental Fig. 4B). In both expression vectors, a CAG promoter drives expression of a bicistronic transcript containing an internal ribosomal entry site (IRES) and *mRFP* fused to *Histone H2B* (pCI-IRES-H2B-RFP*;* Williams et al., 2018). These constructs were electroporated onto the right side of HH4 embryos. Transfected embryos that efficiently expressed H2B-RFP were identified and immunostained with HNK-1 antibody for phenotype analysis. The results revealed a reduction of HNK-1-positive cells in the cardiac stream similar to that seen with MafB MO (Fig.

3I-L and Supplemental Fig. 4B), whereas electroporation of the reporter alone produced no phenotype (Fig. 3G-H). Taken together, these results indicate that MafB is required for proper cardiac neural crest development.

Effects of MafB loss on other cardiac neural crest genes

To examine the role of *MafB* in the cardiac neural crest gene regulatory network, we examined the effects of MafB knockdown on expression of other neural crest transcription factors. To this end, embryos were electroporated with MafB or control MO on the right side and allowed to develop until stage HH12 prior to in situ hybridization with the neural crest markers *Sox10, Krox20, Ets1* as well as *MafB* itself. Embryos electroporated with control MO showed no or few differences between right and left sides (Fig. 4B,E,H,K and Supplemental Fig. 4B). In contrast, expression of *Sox10* was reduced in the cardiac crest stream on the knockdown side of embryos treated with MafB MO, whereas cranial neural crest cells were unaffected (Fig. 4C and Supplemental Fig. 4). Expression of *Krox20, Ets1* and *MafB* itself was also reduced (Fig. 4F,I,L and Supplemental Fig. 4B). Similarly, embryos transfected with *MafB* dominant negative constructs exhibited similar loss of *Sox10*, *Krox20* and *MafB* on the knockdown side, whereas embryos electroporated with the empty vector showed no effect (Supplemental Figs. 4B and 5). Cumulatively, these results show that *MafB* is important for gene expression in the early migrating cardiac neural crest.

Given the advent of CRISPR-Cas9 technology for loss of function analysis, we used CRISPR-Cas9 plasmid constructs previously optimized for electroporation in chicken embryos (Gandhi et al., 2017) to induce mutations in the *MafB* locus. For this purpose, we designed two guide RNAs (gRNAs), one targeting the start codon of MafB, and the second targeting an internal region of its first exon (Fig. 4A). Constructs bearing MafB gRNAs and Cas9 were co-electroporated into the right side of stage HH4 embryos while control gRNA and Cas9 were co-electroporated on the left side of the same embryo. We then examined the effects of genome editing of *MafB* locus on the expression of aforementioned neural crest genes. Analogous to the phenotype observed with the MafB MO, expression of all genes tested was reduced in migrating

cardiac neural crest cells on the knockout side, when compared to the contralateral internal control (Fig. 4D,G,J,M). In contrast, CRISPR-mediated loss of MafB caused no effect on the FoxD3 NC2 enhancer, suggesting a requirement during migration but not induction of the cardiac NC population (Supplemental Fig. 6).

MafB is critical for Sox10E2 enhancer activity in the cardiac neural crest

Sox10 is a neural crest marker gene expressed at all axial levels including the cardiac neural crest. The Sox10E2 enhancer is specifically expressed in the cranial plus post-otic neural crest, but absent from the trunk neural crest (Betancur et al., 2010). To verify expression driven by this enhancer in the cardiac neural crest, we electroporated Sox10E2:EGFP reporter into HH4 chick embryos. Reporter expression was observed in the cardiac neural crest stream at HH12 (Fig. 5B), indicating that cardiac neural crest cells express inputs for Sox10E2 activity.

Previous work has shown that Ets1, cMyb and Sox9 are direct activators of this enhancer at cranial levels (Betancur et al., 2010). To test whether MafB is an input for Sox10E2 enhancer activity in the cardiac neural crest, we used double-sided electroporations, in which Sox10E2:GFP was injected on both sides and control reagents were injected onto the left side of the embryo, to examine the effects of MafB dominant negative constructs and CRISPR-mediated loss of *MafB* on the ability of the enhancer to drive reporter expression (Fig. 5A). For the latter, plasmids driving ubiquitous expression of Cas9, gRNAs and H2B-RFP reporter were co-electroporated. In both cases, loss of *MafB* caused a marked reduction in reporter expression compared with control side, suggesting requirement for Sox10E2 activity in the cardiac neural crest stream (Fig. 5C,D).

The transcription factors *Sox10, Ets1, MafB and Krox20* are concomitantly expressed in migrating cardiac neural crest cells (Fig. 6A-D), whereas *Sox10* is also expressed in other neural crest populations and *Ets1* in cranial and vagal neural crest cells (Fig. 6E). Interestingly, analysis of putative binding motifs using JASPAR (Mathelier et al., 2014) revealed three previously unrecognized putative MafB binding sites within the Sox10E2 enhancer (Fig. 6F), adding to sites already described for Ets1, cMyb and SoxE factors (Betancur et al., 2010). To test the necessity

of MafB sites to mediate reporter expression, we individually mutated each motif within the enhancer. Wild-type or mutant constructs driving GFP were electroporated onto of HH4 chicken embryos together with wild-type Sox10E2 driving mCherry as a control reporter. Mutation of binding motifs MafB(b) and MafB(c) resulted in reduced GFP expression in cardiac neural crest cells at HH12 (Fig. 7D-I). In contrast, mutation of binding motif MafB(a) showed no reduction in GFP expression (Fig. 7A-C). These results suggest that the MafB(b) and MafB(c) binding sites within Sox10E2 contribute to driving reporter expression in the migrating cardiac neural crest cells. Taken together with our loss-of-function results, this suggests that MafB is a critical input for Sox10E2-driven *Sox10* expression in the cardiac neural crest.

DISCUSSION

The cardiac neural crest is a unique cell population with the ability to contribute to critical components of the cardiac outflow tract and other cardiovascular derivatives. Interposed between the cranial and trunk neural crest, cardiac crest cells have an inherently different developmental potential than other neural crest populations. To isolate a pure population of cardiac neural crest cells, we took advantage of the fact that different enhancers mediate expression of the same factor at different levels of the body axis. Whereas the enhancer NC1 drives expression of the *FoxD3* gene in the cranial neural crest, the enhancer NC2 mediates *FoxD3* expression in the cardiac and trunk neural crest (Simões-Costa et al., 2012). A similar situation has been described for another neural crest gene, *Sox10*, which has separate cranial and trunk enhancers. However, the caudal limit of the cranial *FoxD3* enhancer is above the ear, whereas the *Sox10* cranial enhancer, Sox10E2, mediates expression in both the cranial and the post-otic region. Here we show that both *FoxD3* NC2 and Sox10E2 enhancers are active in the cardiac neural crest; indeed, the region of overlap in the expression mediated by the “cranial” *Sox10* enhancer and the “trunk” *FoxD3* enhancer, defines the location of the cardiac neural crest.

To gain insight into the molecular basis of the differences between cardiac and other neural crest populations, we performed genome-wide transcriptional profiling of a pure population

of early migrating cardiac neural crest cells, using a neural crest specific enhancer. Our transcriptome analysis has led to discovery of numerous genes, including transcription factors and signaling molecules that are enriched in the cardiac neural crest and may imbue these cells with their unique properties. The results suggest that the cardiac neural crest has an overall transcriptional signature that is highly reminiscent of the cranial neural crest, with genes like *Ets1* shared between the two populations. Perhaps the fact that the "cranial" Sox10E2 enhancer drives expression in the cardiac neural crest partially explains the overlap between cranial and cardiac neural crest genes. While *Ets1* is cranial/vagal specific, other critical neural crest genes like *Sox10* and *FoxD3* are expressed in all neural crest populations along the body axis.

In addition to shared gene expression, there are also important transcriptional and signaling differences between the cardiac and other neural crest populations. For example, we found several transcription factors, including *MafB* and *Krox20,* selectively expressed in migrating cardiac crest cells but absent from other neural crest populations. Similarly, the receptor *Ret* was highly enriched in this cell population. These findings are consistent with previous reports of Ret in the vagal crest, which overlaps with cardiac neural crest (Natarajan et al., 2002). In the hindbrain, *MafB* and *Krox20* have been well-studied and both are critical for normal patterning of the rhombomeres (Frohman et al., 1993; McKay et al., 1994; Schneider-Maunoury et al., 1993; Seitanidou et al., 1997). However, their expression and role in the cardiac neural crest has not been explored. Recently, Odelin et al. reported that Krox20-expressing neural crest cells populate the aortic valve in mice and that loss of *Krox20* results in abnormal hypertrophic valves (Odelin et al., 2017). Although no heart defects have been reported in *Kreisler* mutant mice which are hypomorphic for *MafB* (Eichmann et al., 1997), the glossopharyngeal ganglion and nerve and the abducens nerve, which are the derivatives of neural crest cells from rhombomeres 5 or 6, are absent (McKay et al., 1994).

Our functional studies show that *MafB* is important during cardiac neural crest development and likely to be a critical component of a cardiac specific gene regulatory subcircuit. After MafB knockdown, we observed a reduction of *Sox10*, *Krox20,* and *MafB* itself. We propose that *MafB* expression in the cardiac neural crest is derived from initial expression in rhombomeres

5/6, then maintained during cardiac neural crest migration by positive autoregulation. Such autoregulation has previously been observed in hindbrain (Giudicelli et al., 2003). A similar autoregulation has been proposed for expression of *Krox20* in rhombomere 5 and the rhombomere 5-derived neural crest cells. The model has two steps: initial *Krox20* expression is activated in rhombomere 5 by hindbrain initiator elements; this is followed by maintenance of *Krox20* expression in the neural crest by cis-acting enhancer elements activated by Krox20 itself and Sox10 (Ghislain et al., 2003). Although transcriptional regulation of *MafB* in the cardiac neural crest remains unexamined, given their co-expression in this cell population and the fact that loss of MafB causes reduced *Krox20* expression, it will be interesting to test if there is cross-regulation, direct or indirect, between *MafB* and *Krox20*.

Our results reveal a new role for MafB in regulating *Sox10* expression. The Sox10E2 enhancer drives specific expression in the cranial/vagal neural crest and the otic vesicle. Here we confirmed that the enhancer is also active in the cardiac neural crest cells and that it contains three putative MafB binding sites. Mutational analysis further revealed that removal of sites MafB(b) or MafB(c) reduces Sox10E2 reporter activity. This suggests that MafB may be a direct input into the expression of *Sox10* gene. Previously, Ets1 has been shown to directly regulate this same Sox10E2 enhancer (Betancur et al., 2010). As MafB has been shown to interact with Ets1 in the hematopoietic system (Sieweke et al., 1996), we speculate that MafB and Ets1 may function in a transcriptional complex to directly activate Sox10E2 in the cardiac neural crest population (Fig. 6G).

Previous loss of function studies in mouse (Gao et al., 2010; Ye et al., 2009) and Xenopus (Nie and Bronner, 2015) have shown that Ets1 plays an important role in cardiovascular development. Although *Ets1* is expressed in both the cranial and cardiac neural crest, its loss of function appears to have a primary effect on the cardiac neural crest. For example, a mutation in the human *Ets1* gene (Grossfeld et al., 2004) results in Jacobsen syndrome, characterized by septation defects that are reminiscent of cardiac neural crest ablation in the chick. By contrast, craniofacial defects in these patients are absent or minor. Similarly, *Ets1* knockout mice have large membranous interventricular septal defects in the absence of other structural heart defects

(Ye et al., 2009). This may suggest that the primary role of Ets1 may be in the cardiac neural crest. It is intriguing to speculate that *MafB* may have a role in conferring a "cardiac" identity onto *Ets1*-expressing neural crest cells. If so, addition of *MafB* may be sufficient to confer a cardiac crest identify onto other neural crest populations differentiated from ES and/or iPS cells, thus leading to a better understanding of the etiology of cardiac-crest related defects.

Taken together, we propose that *MafB* is part of a gene regulatory subcircuit that is unique to the cardiac neural crest (Fig. 6G). Together with previous evidence suggesting a critical role for Ets1, we propose that MafB and Ets1 may work together in the cardiac neural crest to activate important neural crest genes like *Sox10*. *MafB* appears to be upstream of *Sox10* and *Krox20* and to positively autoregulate its expression. Future experiments testing the role of other cardiac specific transcription factors hold the promise of further elaborating this cardiac neural crest specific gene regulatory circuit.

MATERIALS AND METHODS

Embryos and electroporation

Fertilized chicken eggs were obtained from commercial farms (U.S.A. or Japan) and incubated at 37°C to the desired HH stage (Hamburger and Hamilton, 1951). Electroporations were performed *ex ovo* at stage HH4 as previously described (Sauka-Spengler and Barembaum, 2008), using 5 pulses of 5.2V for 50 ms with 100 ms intervals. After electroporation, embryos were cultured at 37°C on albumin-coated dishes until HH12. DNA concentration in injected solutions was 1.5 µg/µL for plasmids encoding gRNAs or 2 µg/µL for all other plasmids. MOs were electroporated at 1-1.5 mM.

Tissue dissociation and cell sorting

Embryos electroporated with pTK(NC2:EGFP) (Simões-Costa et al., 2012) were incubated until stage HH12 and had tissue from the region between the otic vesicle and the 3rd somite dissected and dissociated with Accumax (Innovative Cell Technologies, Inc.). Dissociated cells were prepared for fluorescence activated sorting as previously described (Simões-Costa et

al., 2014). GFP+ and GFP- cells were sorted using the BD FACSAria Cell Sorter (BD Biosciences).

RNA sequencing and analysis

RNA was extracted from the sorted cells with RNAqueous-Micro Kit (Ambion) and libraries were prepared with the Ovation RNA-Seq System V2 (NuGEN). Three biological replicates of GFP+ and GFP- cells, each one pooled from several embryos, were sequenced on the Illumina HiSeq2500 platform. The sequenced reads were mapped to the chicken genome (galGal5) using HISAT2 (Kim et al., 2015) and read counts per gene were calculated using featureCounts (Liao et al., 2014). Differential gene expression analysis was performed using DESeq2 (Love et al., 2014) and genes with adjusted p-value below 0.05 were considered to be differentially expressed. Protein classification analysis was performed using PANTHER (Thomas, et al., 2003). Functional annotation clustering was performed using DAVID and human genome annotations (Huang et al., 2009).

cDNA synthesis

Total RNA was extracted with RNAqueous Kit (Ambion) from HH11-12 embryos and cDNA was synthesized with SuperScript III (Invitrogen). Gene fragments were amplified with Phusion High Fidelity PCR Kit (New England BioLabs).

***In situ* hybridization**

RNA probes were synthesized with DIG-RNA labeling mix (Roche) and SP6 promoter or T7 RNA polymerases (Promega). Templates for *Cxcr4*, *Nrip* and *MafB* probes were amplified with primers listed in Supplemental Table 3 and cloned into pGEM-T (Promega) or TOPO TA (Invitrogen) vectors. Two templates for MafB were used: the entire coding sequence, amplified with MafB-Fw1 and MafB-Rv1 and used for WT or MO-electroporated embryos, or the N-terminal coding region (1-194 aa), amplified with MafB-Fw1 and MafB-Rv2 and used for embryos electroporated with MafB dominant negative constructs. Templates for *Dlx5, Msx1*, *Ret*, *TFAP2A* and *Ets1* were EST clones (BBSRC ChickEST Database) and templates for *LBH*, *LTK*, *Mef2C*,

RXRG, *Slit1*, *Snail2*, *Sox10* and *TFAP2B* were previously described (Giudicelli et al., 2001; Simões-Costa et al., 2014). Whole mount in situ hybridization was performed as previously described (Acloque et al., 2008). Fluorescence in situ hybridization was performed with the TSA Plus Cyanine 3/Fluorescein Kit (PerkinElmer).

Immunostaining

Embryos were fixed with 4% paraformaldehyde, washed three times with 0.2% Triton X-100 and 0.1% DMSO in PBS and blocked with 10% donkey serum diluted in the same solution. The following primary antibodies were used: anti-HNK-1 (DSHB Cat# 3H5, RRID:AB_2314644; 1:10), anti-GFP (Thermo Fisher Scientific Cat# A-11122, RRID:AB_221569 or Abcam Cat# ab6673, RRID:AB_305643; 1: 100 or 1:1000, respectively), anti-mCherry (MBL International Cat# PM005, RRID:AB_591279; 1:1000). The secondary antibodies were donkey anti-rabbit IgG, donkey anti-mouse IgG or goat anti-mouse IgM conjugated with Alexa Fluor 488/594 (Molecular Probes Cat# A-11055, RRID:AB_142672; Cat# A-21207, RRID:AB_141637; Cat# A-21042, RRID:AB_141357; Cat# A-21044, RRID:AB_141424; 1:2000). DAPI was used for nuclei counterstaining.

Histology

Stained embryos were cryoprotected with sequential immersion in 5% and 15% sucrose in PBS until equilibrated, followed by infiltration with 7.5% gelatin for at least 3 hours at 37°C. The embryos were embedded into gelatin and frozen in liquid nitrogen. Sections of 10-20 μm were obtained using a Microm cryostat (HM550). After sectioning and prior to mounting, gelatin was removed from slides by soaking in PBS at 37°C for 15 min.

Loss-of-function studies

MafB and standard control MOs were purchased from Gene Tools. To create the empty vector pCI-FLAG-H2B-RFP, the oligos FLAG-Fw and FLAG-Rv (Supplemental Table 3) were annealed and inserted into pCI-IRES-H2B-RFP digested with XhoI and SphI. To create pCI-(FLAG-MafBΔN-H2B-RFP), MafBΔN was amplified with the primers MafB-Fw2 and

MafB-Rv3 (Supplemental Table 3) and cloned into pCI-FLAG-IRES-H2B-RFP. To create pCI-(FLAG-MafBΔN-EnR-H2B-RFP), the Engrailed repressor domain was inserted into pCI-FLAG-MafBΔN-H2B-RFP after removal of the stop codon of MafBΔN. CRISPR-mediated loss of *MafB* was performed using pCAG(NLS-Cas9-NLS) and cU6.3 plasmids to drive expression of control or targeted gRNA, co-electroporated with pCI(H2B-RFP) to ensure efficient transfection of the embryos analyzed (Gandhi et al., 2017). The genomic locus of MafB was obtained from UCSC genome browser (Kent et al., 2002). MafB.1.gRNA (5'-GCCCGCAAGACAGCGATGGC-3') and MafB.2.gRNA (5'-GGAGCCGATGAGGGCTTCGA-3') were designed using the CRISPR-design tool available at http://crispr.mit.edu. For effects on the Sox10E2 enhancer, knock-down reagents were co-electroporated with pTK(Sox10E2:EGFP) (Betancur et al., 2010).

Binding motif analysis

MafB binding motifs were predicted using JASPAR database (Mathelier et al., 2014). Mutated Sox10E2 fragments were created with the KOD Kit (Takara), using primers for amplifying Sox10E2 combined with primers designed to introduce MafB(a), MafB(b), or MafB(c) (Supplemental Table 3) mutations, and cloned into KpnI/XhoI sites of pTK-EGFP (Uchikawa et al., 2003).

ACKNOWLEDGEMENTS

We thank Dr. Patrick Charnay for the chicken *Krox20* probe and the Caltech Flow Cytometry and Genomics Facilities for technical support. This work was supported by Toyobo Biotechnology Foundation postdoctoral fellowship and Japan Society for the Promotion of Science KAKENHI JP16K18551 to STM, National Institutes of Health R01DE024157 and RO1HL140587 to MEB and a postdoctoral fellowship from the Curci Foundation to FMV.

Supplemental Figure 1. Neural crest expression of selected genes enriched in post-otic NC2+ sorted cells. (A-F) Transverse sections of HH12/13 embryos stained with in situ hybridization showing expression in the migratory cardiac neural crest, identified with HNK-1 immunostaining in (D-F).

Supplemental Figure 2. *MafB* is specifically expressed in the hindbrain and cardiac neural crest. (A-C) In situ hybridization showing *MafB* expression in HH10 (A) and HH13 (B-C) embryos; (C) is a transverse section of the embryo shown in (B).

Supplemental Figure 3. MafB MO blocks translation of *MafB* transcript. (A) Diagram showing the reporter construct designed to test activity of MafB MO, where the MafB 5' untranslated region (UTR) and partial coding sequence, containing the MO target, were fused in frame with the *RFP* coding sequence. (B) Diagram showing double-sided co-electroporation of the reporter construct with MafB MO on the right side or a control MO on the left side. (C-E) Immunostaining showing successful delivery of FITC-tagged MOs on both sides (C) and specific loss of RFP reporter on MafB-depleted side. White dashed lines indicate the midline.

Supplemental Figure 4. Effects of MafB loss on expression of neural crest markers. (A) In situ hybridization for *Sox10* after MAFB MO electroporation showing examples of none, mild, strong or severe phenotypes. Gray and black arrowheads point to wild-type and MafB-depleted cardiac neural crest streams, respectively. (B) Barplots for the qualitative classification based on severity of the phenotype after electroporation of control or MafB loss-of-function reagents, as assessed by immunostaining with HNK-1 or in situ hybridization for *Sox10*, *MafB*, *Krox20* or *Ets1*. n: number of embryos analyzed per condition.

Supplemental Figure 5. MafBΔN-EnR causes loss of cardiac neural crest markers. (A-F) In situ hybridization for *Sox10* (A-B), *MafB* (C-D) or *Krox20* (E-F) in HH12 embryos after empty vetor (A,C,E) or MAFBΔN-EnR (B,D,F) electroporation at HH4, showing down-regulation of these markers in MafB-depleted cardiac neural streams. White, gray and black arrowheads point to wild-type, control and MafB-depleted cardiac neural crest streams, respectively.

Supplemental Figure 6. MafB is not required for NC2 enhancer activity. (A) NC2-driven mCherry expression in HH12 embryos electroporated with NC2:mCherry on both sides together with control or MafB gRNAs on either side of the embryo, showing no reduction in NC2-driven expression after loss of MafB. Gray and yellow arrowheads point to control and MafB-depleted cardiac neural crest streams, respectively. The dashed white line indicate the midline.

REFERENCES

Acloque, H., Wilkinson, D.G., Nieto, M.A., 2008. Chapter 9 In Situ Hybridization Analysis of Chick Embryos in Whole-Mount and Tissue Sections, in: Methods in Cell Biology. pp. 169–185. https://doi.org/10.1016/S0091-679X(08)00209-4

Besson, W.T., Kirby, M.L., Van Mierop, L.H.S., Teabeaut, J.R., 1986. Effects of the size of lesions of the cardiac neural crest at various embryonic ages on incidence and type of cardiac defects. Circulation 73, 360–364. https://doi.org/10.1161/01.CIR.73.2.360

Betancur, P., Bronner-Fraser, M., Sauka-Spengler, T., 2010. Genomic code for Sox10 activation reveals a key regulatory enhancer for cranial neural crest. Proc. Natl. Acad. Sci. U. S. A. 107, 3570–3575. https://doi.org/10.1073/pnas.0906596107

Conlon, F.L., Sedgwick, S.G., Weston, K.M., Smith, J.C., 1996. Inhibition of Xbra transcription activation causes defects in mesodermal patterning and reveals autoregulation of Xbra in dorsal mesoderm 2435, 2427–2435.

Eichmann, A., Grapin-Botton, A., Kelly, L., Graf, T., Le Douarin, N.M., Sieweke, M., 1997. The expression pattern of the mafB/kr gene in birds and mice reveals that the kreisler phenotype does not represent a null mutant. Mech. Dev. 65, 111–122. https://doi.org/10.1016/S0925-4773(97)00063-4

Escot, S., Blavet, C., Härtle, S., Duband, J.L., Fournier-Thibault, C., 2013. Misregulation of SDF1-CXCR4 signaling impairs early cardiac neural crest cell migration leading to conotruncal defects. Circ. Res. 113, 505–516. https://doi.org/10.1161/CIRCRESAHA.113.301333

Frohman, M. a, Martin, G.R., Cordes, S.P., Halamek, L.P., Barsh, G.S., 1993. Altered rhombomere-specific gene expression and hyoid bone differentiation in the mouse segmentation mutant, kreisler (kr). Development 117, 925–936.

Gandhi, S., Piacentino, M.L., Vieceli, F.M., Bronner, M.E., 2017. Optimization of CRISPR/Cas9 genome editing for loss-of-function in the early chick embryo. Dev. Biol. 432, 86–97. https://doi.org/10.1016/j.ydbio.2017.08.036

Gao, Z., Kim, G.H., Mackinnon, A.C., Flagg, A.E., Bassett, B., Earley, J.U., Svensson, E.C., 2010. Ets1 is required for proper migration and differentiation of the cardiac neural crest. Development 137, 1543–1551. https://doi.org/10.1242/dev.047696

Ghislain, J., Desmarquet-Trin-Dinh, C., Gilardi-Hebenstreit, P., Charnay, P., Frain, M., 2003. Neural crest patterning: autoregulatory and crest-specific elements co-operate for Krox20 transcriptional control. Development 130, 941–953. https://doi.org/10.1242/dev.00318

Giudicelli, F., Taillebourg, E., Charnay, P., Gilardi-Hebenstreit, P, 2001. Krox-20 patterns the hindbrain through both cell-autonomous and non cell-autonomous mechanisms. Genes Dev. 15:567-580.

Giudicelli, F., Gilardi-Hebenstreit, P., Mechta-Grigoriou, F., Poquet, C., Charnay, P., 2003. Novel activities of Mafb underlie its dual role in hindbrain segmentation and regional specification. Dev. Biol. 253, 150–162. https://doi.org/10.1006/dbio.2002.0864

Grossfeld, P.D., Mattina, T., Lai, Z., Favier, R., Jones, K.L., Cotter, F., Jones, C., 2004. The 11q terminal deletion disorder: A prospective study of 110 cases. Am. J. Med. Genet. 129A, 51–61. https://doi.org/10.1002/ajmg.a.30090

Hamburger, V., Hamilton, H.L., 1951. A series of normal stages in the development of the chick embryo. J. Morphol. 88, 49–92. https://doi.org/10.1002/jmor.1050880104

Huang da, W., Sherman, B.T., Lempicki, R.A., 2009. Systematic and integrative analysis of large gene lists using DAVID bioinformatics resources. Nat. Protoc. 4:44-57.

Hutson, M.R., Kirby, M.L., 2007. Model systems for the study of heart development and disease. Cardiac neural crest and conotruncal malformations. Semin. Cell Dev. Biol. https://doi.org/10.1016/j.semcdb.2006.12.004

Kent, W.J., Sugnet, C.W., Furey, T.S., Roskin, K.M., Pringle, T.H., Zahler, A.M., Haussler, D., 2002. The human genome browser at UCSC. Genome Res. 12:996-1006.

Kim, D., Langmead, B., Salzberg, S.L., 2015. HISAT: A fast spliced aligner with low memory requirements. Nat. Methods 12, 357–360. https://doi.org/10.1038/nmeth.3317

Kirby, M.L., 1989. Plasticity and predetermination of mesencephalic and trunk neural crest transplanted into the region of the cardiac neural crest. Dev. Biol. 134, 402–412. https://doi.org/10.1016/0012-1606(89)90112-7

Kirby, M.L., Gale, T.F., Stewart, D.E., 1983. Neural crest cells contribute to normal aorticopulmonary septation. Science (80-.). 220, 1059–61. https://doi.org/10.1126/science.6844926

Kirby, M.L., Stewart, D.E., 1983. Neural crest origin of cardiac ganglion cells in the chick embryo: Identification and extirpation. Dev. Biol. 97, 433–443. https://doi.org/10.1016/0012-1606(83)90100-8

Kirby, M.L., Turnage, K.L., Hays, B.M., 1985. Characterization of conotruncal malformations following ablation of “cardiac” neural crest. Anat. Rec. 213, 87–93. https://doi.org/10.1002/ar.1092130112

Le Douarin, N.M., 1982. The Neural Crest. Cambridge Univ. Press.

Le Lièvre, C.S., Le Douarin, N.M., 1975. Mesenchymal derivatives of the neural crest: analysis of chimaeric quail and chick embryos. J. Embryol. Exp. Morphol. 34, 125–154.

Lecoin, L., Sii-Felice, K., Pouponnot, C., Eychène, A., Felder-Schmittbuhl, M.P., 2004. Comparison of maf gene expression patterns during chick embryo development. Gene Expr. Patterns 4, 35–46. https://doi.org/10.1016/S1567-133X(03)00152-2

Liao, Y., Smyth, G.K., Shi, W., 2014. FeatureCounts: An efficient general purpose program for assigning sequence reads to genomic features. Bioinformatics 30, 923–930. https://doi.org/10.1093/bioinformatics/btt656

Love, M.I., Huber, W., Anders, S., 2014. Moderated estimation of fold change and dispersion for RNA-seq data with DESeq2. Genome Biol. 15, 1–21. https://doi.org/10.1186/s13059-014-0550-8

Mathelier, A., Zhao, X., Zhang, A.W., Parcy, F., Worsley-Hunt, R., Arenillas, D.J., Buchman, S., Chen, C.Y., Chou, A., Ienasescu, H., Lim, J., Shyr, C., Tan, G., Zhou, M., Lenhard, B., Sandelin, A., Wasserman, W.W., 2014. JASPAR 2014: An extensively expanded and updated open-access database of transcription factor binding profiles. Nucleic Acids Res. 42, 142–147. https://doi.org/10.1093/nar/gkt997

McKay, I.J., Muchamore, I., Krumlauf, R., Maden, M., Lumsden, A., Lewis, J., 1994. The kreisler mouse: a hindbrain segmentation mutant that lacks two rhombomeres. Development 120, 2199–2211.

Meulemans, D., Bronner-Fraser, M., 2004. Gene-regulatory interactions in neural crest evolution and development. Dev. Cell 7, 291–299. https://doi.org/10.1016/j.devcel.2004.08.007

Natarajan, D., Marcos-Gutierrez, C., Pachnis, V., de Graaff, E., 2002. Requirement of signalling by receptor tyrosine kinase RET for the directed migration of enteric nervous system progenitor cells during mammalian embryogenesis. Development 129, 5151–5160.

Neeb, Z., Lajiness, J.D., Bolanis, E., Conway, S.J., 2013. Cardiac outflow tract anomalies. Wiley Interdiscip. Rev. Dev. Biol. https://doi.org/10.1002/wdev.98

Nie, S., Bronner, M.E., 2015. Dual developmental role of transcriptional regulator Ets1 in Xenopus cardiac neural crest vs. heart mesoderm. Cardiovasc. Res. 106, 67–75. https://doi.org/10.1093/cvr/cvv043

Nishibatake, M., Kirby, M.L., Van Mierop, L.H.S., 1987. Pathogenesis of persistent truncus arteriosus and dextroposed aorta in the chick embryo after neural crest ablation. Circulation 75, 255–264. https://doi.org/10.1161/01.CIR.75.1.255

Odelin, G., Faure, E., Coulpier, F., Di Bonito, M., Bajolle, F., Studer, M., Avierinos, J.-F., Charnay, P., Topilko, P., Zaffran, S., 2017. Krox20 defines a subpopulation of cardiac neural crest cells contributing to arterial valves and bicuspid aortic valve. Development. https://doi.org/10.1242/dev.151944

Schneider-Maunoury, S., Topilko, P., Seitanidou, T., Levi, G., Cohen-Tannoudji, M., Pournin, S., Babinet, C., Charnay, P., 1993. Disruption of Krox-20 results in alteration of rhombomeres 3 and 5 in the developing hindbrain. Cell 75, 1199–1214. https://doi.org/10.1016/0092-8674(93)90329-O

Seitanidou, T., Schneider-Maunoury, S., Desmarquet, C., Wilkinson, D.G., Charnay, P., 1997. Krox-20 is a key regulator of rhombomere-specific gene expression in the developing hindbrain. Mech. Dev. 65, 31–42. https://doi.org/10.1016/S0925-4773(97)00051-8

Sieweke, M.H., Tekotte, H., Frampton, J., Graf, T., 1996. MafB is an interaction partner and repressor of Ets-1 that inhibits erythroid differentiation. Cell 85, 49–60. https://doi.org/10.1016/S0092-8674(00)81081-8

Simoes-Costa, M., Bronner, M.E., 2016. Reprogramming of avian neural crest axial identity and cell fate. Science (80-.). 352, 1570–1573. https://doi.org/10.1126/science.aaf2729

Simões-Costa, M., Bronner, M.E., 2015. Establishing neural crest identity: a gene regulatory recipe. Development 142, 242–57. https://doi.org/10.1242/dev.105445

Simões-Costa, M., Tan-cabugao, J., Antoshechkin, I., Sauka-spengler, T., Bronner, M.E., 2014. Transcriptome analysis reveals novel players in the cranial neural crest gene regulatory network. Genome Res. 281–290. https://doi.org/10.1101/gr.161182.113

Simões-Costa, M.S., McKeown, S.J., Tan-Cabugao, J., Sauka-Spengler, T., Bronner, M.E., 2012. Dynamic and Differential Regulation of Stem Cell Factor FoxD3 in the Neural Crest Is Encrypted in the Genome. PLoS Genet. 8. https://doi.org/10.1371/journal.pgen.1003142

Thomas, P.D., Campbell, M.J., Kejariwal, A., Mi, H., Karlak, B., Daverman, R., Diemer, K., Muruganujan, A., Narechania, A., 2003. PANTHER: a library of protein families and subfamilies indexed by function. Genome Res. 13:2129-2141.

Uchikawa, M., Ishida, Y., Takemoto, T., Kamachi, Y., Kondoh, H., 2003. Functional analysis of chicken Sox2 enhancers highlights an array of diverse regulatory elements that are conserved in mammals. Dev. Cell. https://doi.org/10.1016/S1534-5807(03)00088-1

Waldo, K., Miyagawa-Tomita, S., Kumiski, D., Kirby, M.L., 1998. Cardiac neural crest cells provide new insight into septation of the cardiac outflow tract: Aortic sac to ventricular septal closure. Dev. Biol. 196, 129–144. https://doi.org/10.1006/dbio.1998.8860

Williams, R.M., Senanayake, U., Artibani, M., Taylor, G., Wells, D., Ahmed, A.A., Sauka-Spengler, T., 2018. Genome and epigenome engineering CRISPR toolkit for in vivo modulation of cis -regulatory interactions and gene expression in the chicken embryo. Development 145, dev.160333. https://doi.org/10.1242/dev.160333

Ye, M., Coldren, C., Liang, X., Mattina, T., Goldmuntz, E., Benson, D.W., Ivy, D., Perryman, M.B., Garrett-Sinha, L.A., Grossfeld, P., 2009. Deletion of ETS-1, a gene in the Jacobsen syndrome critical region, causes ventricular septal defects and abnormal ventricular morphology in mice. Hum. Mol. Genet. 19, 648–656. https://doi.org/10.1093/hmg/ddp532

Figure 1. RNA-seq analysis of the migrating cardiac neural crest. (A-B) Immunostaining showing GFP reporter expression at stage HH12 (A) in the post-otic region (B), after electroporation at stage HH4; (B) is a higher magnification picture of the embryo shown in (A), the dashed line delimits the axial level isolated for cell sorting. White arrows point to otic vesicle. (C) Immunostaining with HNK-1 of a transverse section confirmed the neural crest identity of GFP-positive cells in the post-otic region (arrowheads). (D) Plot showing fluorescence intensities of cells pooled to form the GFP-positive (blue) and GFP-negative (red) sorted populations. (E) Volcano plot showing differential expression data obtained after comparison of RNA-seq data obtained from GFP+ and GFP- cell populations. (F) Venn diagrams showing overlap of upregulated gene lists obtained for cardiac or cranial (Simões-Costa et al., 2014) neural crest cell

populations. (G) Bar plots showing top hits for annotated genes enriched in the cardiac neural crest, after excluding genes also present in cranial neural crest cells. (H) Classification of proteins encoded by genes upregulated in the cardiac neural crest. (I) GO terms highly associated with cardiac neural crest genes.

Figure 2. Spatial expression pattern of genes enriched in the cardiac neural crest. (A,C-O) In situ hybridization of HH12/13 embryos showing expression in cardiac neural crest streams as seen from dorsal views of whole mount embryos. (B) Double fluorescence in situ hybridization showing overlap between *MafB* and *Krox20* expression in the cardiac neural crest and rhombomere 5 (r5), but not 3 (r3) and 6 (r6), positive for either *Krox20* or *MafB* alone, respectively.

Figure 3. MafB is required in the cardiac neural crest. (A) Diagrams showing position of the MO target in the *MafB* transcript and protein domains in MafB wild-type, acidic-domain truncated (MafBΔN; 194-312 aa) and Engrailed-fused (MafBΔN-EnR) constructs. (B) Diagram showing unilateral *ex ovo* electroporation of HH4 embryos. (C-L) Immunostaining of HH12 embryos for FITC, RFP or HNK-1 after electroporation of control MO (C,D), MafB MO (E-F), H2B-RFP (G,H), MafBΔN (I,J) or MafBΔN-EnR (K,L) showing normal cardiac neural crest streams in embryos transfected with control reagents (D,H) and reduced cardiac neural crest streams after transfection of MafB loss-of-reagents (F,J,L) when compared to contralateral controls (left side). White, gray and yellow arrowheads point to wild-type, control and MafB-depleted cardiac neural crest streams, respectively. Dashed white lines indicate the midline.

Figure 4. MafB is required for expression of cardiac neural crest markers. (A) Diagram showing positions of targets of two MafB gRNAs within the *MafB* gene. (B-M) In situ hybridization for *Sox10* (B-D), *MafB* (E-G), *Krox20* (H-J) or *Ets1* (K-M) of HH12 embryos unilaterally electroporated with control MO (B,E,H,K) or MafB MO (C,F,I,L), or bilaterally electroporated with control and MafB gRNAs (D,G,J,M) showing reduced expression after loss of MafB. White, gray and black arrowheads point to wild-type, control and MafB-depleted cardiac neural crest streams, respectively.

Figure 5. MafB is required for Sox10E2 enhancer activity. (A) Diagram showing double-sided electroporation of control and loss-of-function reagents onto the left and right sides of HH4 embryos, respectively. (B-D) Immunostaining for GFP in HH12 embryos electroporated with Sox10E2:EGFP on both sides alone (B) or together with control or MafB loss-of-function (LOF) constructs on either side of the embryo (C,D), showing loss of Sox10E2-driven expression after loss of MafB. White, gray and yellow arrowheads point to wild-type, control and MafB depleted cardiac neural crest streams, respectively. Dashed white lines indicate the midline.

Figure 6. A model for MafB function in the neural crest. (A-D) In situ hybridization showing expression of *Sox10, Ets1, Krox20* and *MafB* in cranial, cardiac and trunk neural crest axial levels at stage HH12; blue, red and green arrowheads show expression in cranial, cardiac and trunk populations, respectively. (E) Diagram of the neural crest expression patterns of *Sox10, Ets1, Krox20* and *MafB*, represented by separate gray bars: all genes are present in the cardiac population, whereas *Ets1* is expressed in cranial cells and *Sox10* is a marker for the neural crest along the entire neural axis. (F) Diagram showing the position of transcription factor binding sites (colored boxes) in the Sox10E2 sequence, depicting three putative MafB sites (a, b and c) (orange). (G) A model for Sox10E2 activation mediated by binding of MafB and Ets1 to adjacent sites in the Sox10E2 enhancer.

Figure 7. MafB(b) and MafB(c) are required for MafB activation of the Sox10E2 enhancer (E2). (A-I) Immunostaining for mCherry (magenta) and GFP (green) in HH12 embryos electroporated at HH4 to express wild-type Sox10E2-driven GFP on the left side and Sox10E2-MafB(a) (A-C), Sox10E2-MafB(b) (D-F) or Sox10E2-MafB(c) (G-I) on the right side, showing reduced reporter expression driven by Sox10E2-MafB(b) (E-F) and Sox10E2-MafB(c) (H-I) constructs. Gray and yellow arrowheads point to cardiac neural crest stream reporter expression driven by control and mutated constructs, respectively. Dashed white lines indicate the midline. ov: otic vesicle.

HIGHLIGHTS

- We describe the transcriptome of early migrating cardiac neural crest cells.
- We show that the transcription factor MafB is required in migrating cardiac neural crest cells.
- We characterize two biologically relevant MafB binding sites within the Sox10 enhancer Sox10E2.

FIGURE 1

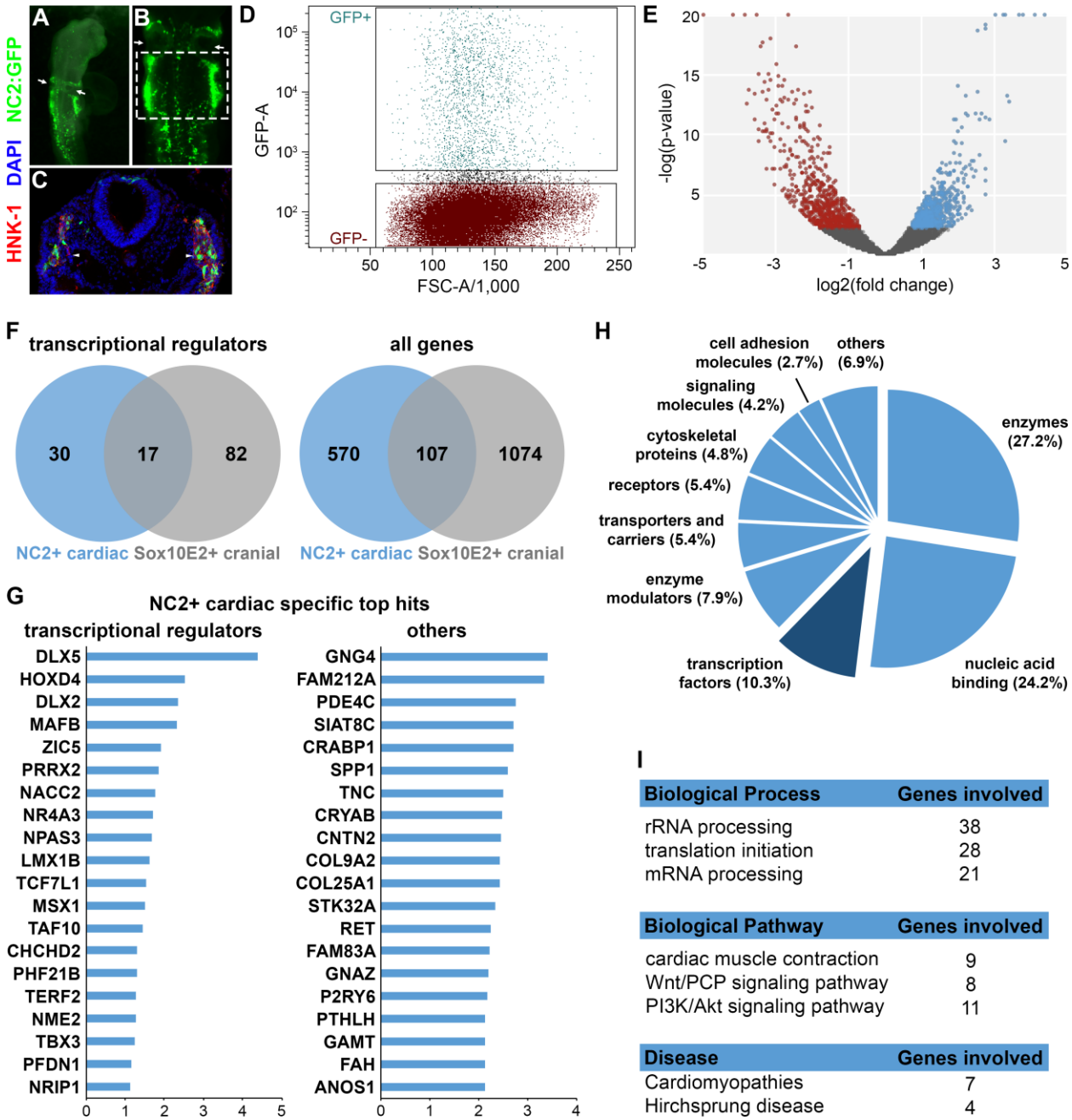

I

Biological Process	Genes involved
rRNA processing	38
translation initiation	28
mRNA processing	21

Biological Pathway	Genes involved
cardiac muscle contraction	9
Wnt/PCP signaling pathway	8
PI3K/Akt signaling pathway	11

Disease	Genes involved
Cardiomyopathies	7
Hirchsprung disease	4

FIGURE 2

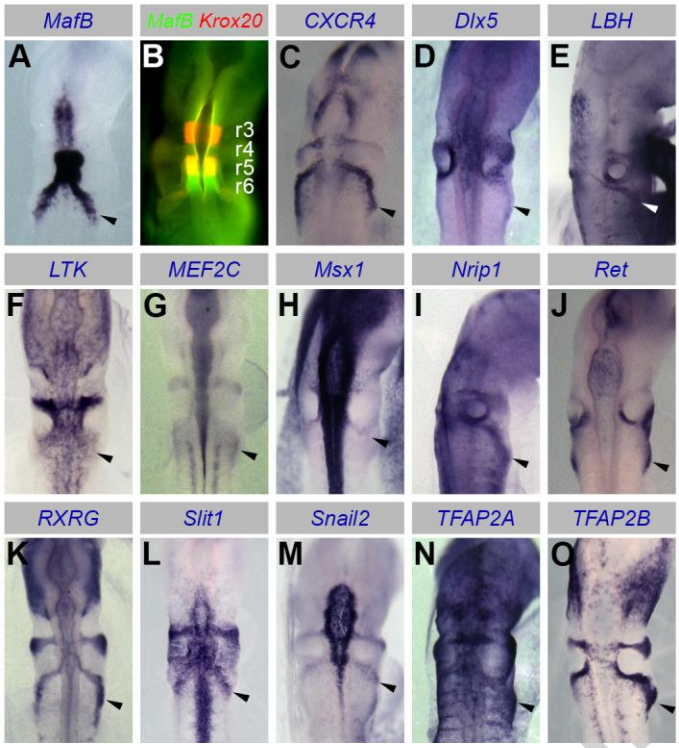

FIGURE 3

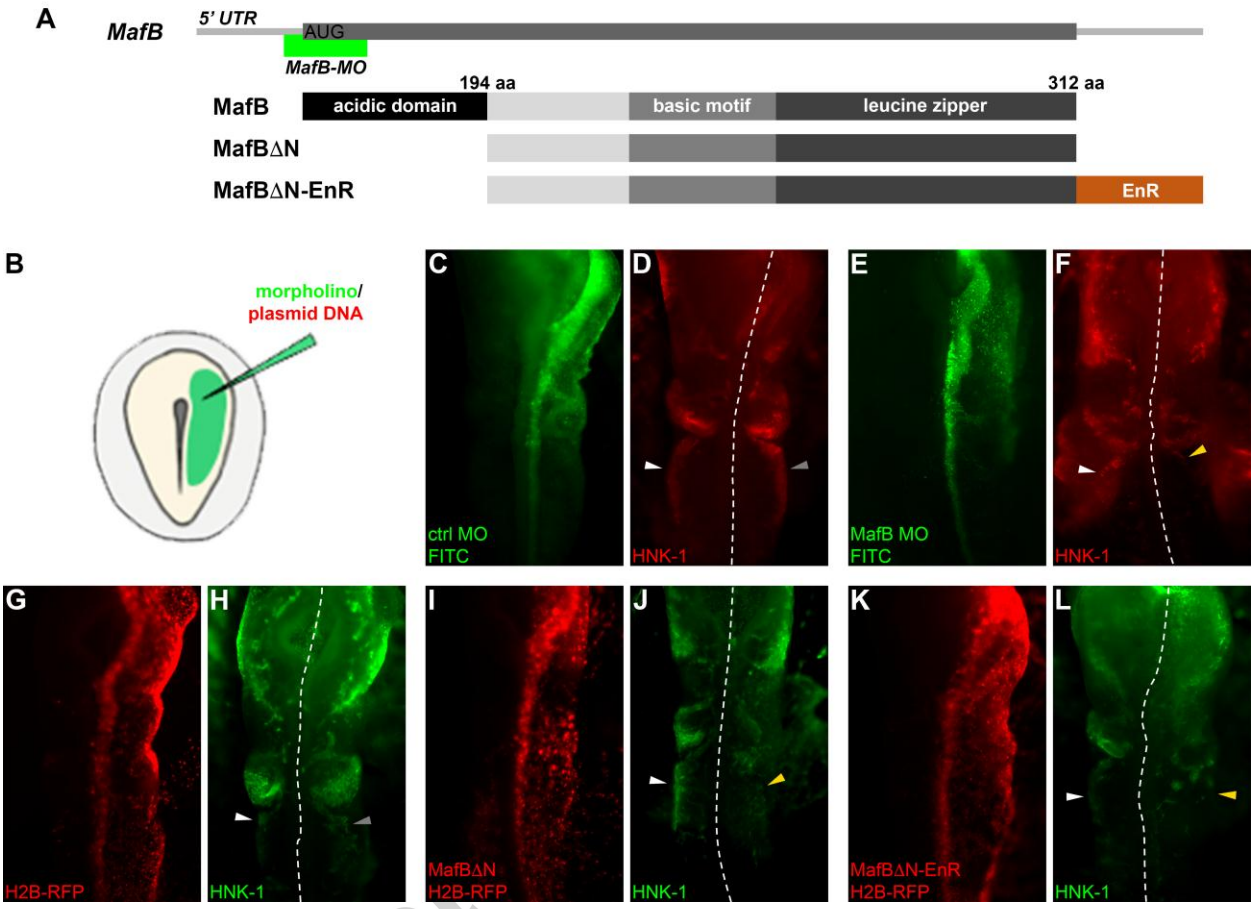

FIGURE 4

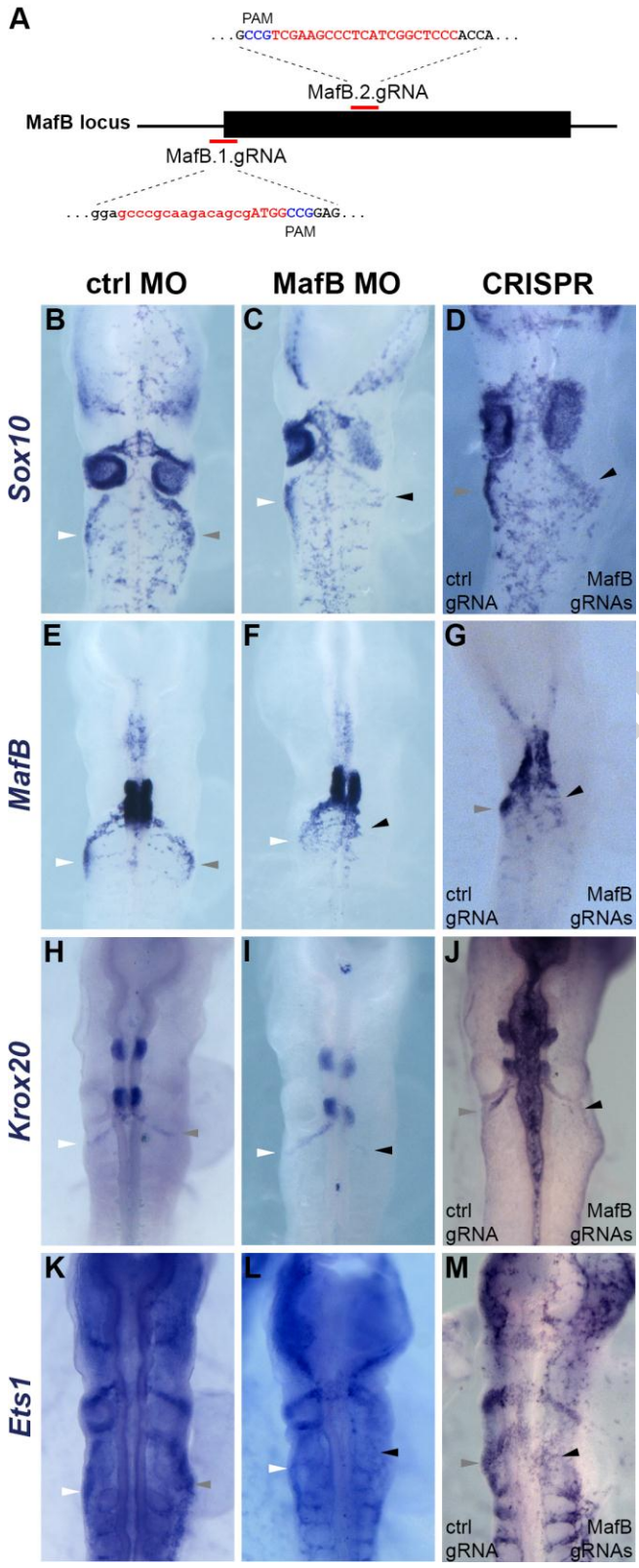

FIGURE 5

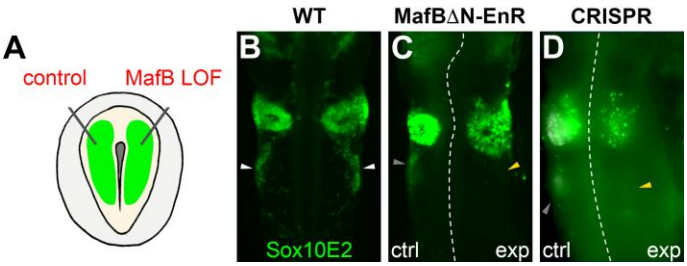

FIGURE 6

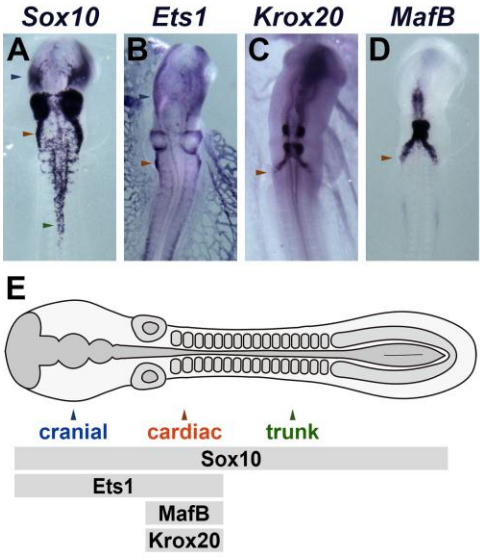

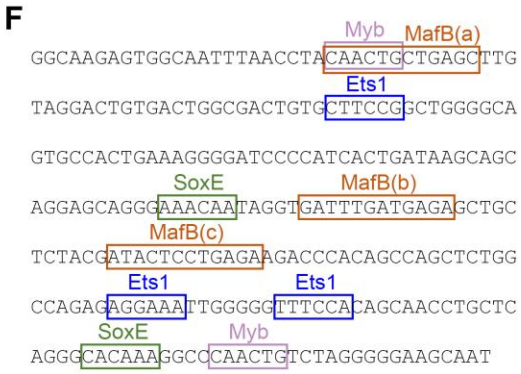

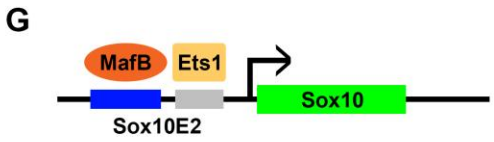

FIGURE 7